Int. J. Electrochem. Sci., 12 **(2017)** 7844 – 7852, doi: 10.20964/2017.08.37

International Journal of
ELECTROCHEMICAL
SCIENCE
www.electrochemsci.org

Short Communication

Preparation and Electrochemical Performance of Coconut Shell Activated Carbon Produced by the H_3PO_4 Activation with Rapid Cooling Method

Ming Zhang[1], *Yonggang Li*[1,*], *Hongyu Si*[2], *Bing Wang*[1], *Tao Song*[1]

[1] College of chemical engineering, Qinghai University, Xining 810016, China
[2] Energy Institute of Shandong Academy of Sciences, Jinan, 250014, China
[*]E-mail: 18209712799@126.com

Received: 2 May 2017 / *Accepted:* 7 June 2017 / *Published:* 12 July 2017

Activated carbon (AC) was prepared by the H_3PO_4 activation of coconut shells. After activation, AC was immediately treated by rapid cooling with liquid nitrogen to prevent the pore occlusion typically observed during natural cooling thereby prevent pore sizes and pore volumes from decreasing. When compared with slow cooling, rapid cooling increased pore sizes from 2.540 nm to 2.936 nm and increased the specific surface area from 578.224 m^2/g to 1176.344 m^2/g. Futhermore, rapid cooling method reduced the number of carboxyl and lactone groups and increased the number of hydroxyl groups. In electrochemical testing, carbon electrodes prepared from the AC showed excellent double-layer capacitance performance, with a substantial increase in specific capacitance from 66.06 F/g to 101.68 F/g and lower impedance.

Keywords: activated carbon; rapid cooling; pore sizes; specific surface area; specific capacitance

1. INTRODUCTION

Electrochemical capacitors, or supercapacitors, have high power density, rapid charge and discharge cycles and longer lifetimes. Because of their outstanding performance, supercapacitors have drawn attention worldwide as a clean energy storage device widely used in many fields [1,2,3].

Activated carbon (AC) is often used as an electrode material for supercapacitors [4], because of its high specific surface area, developed pore structures, excellent adsorption, low cost, abundant raw material sources and simple preparation process [5,6,7]. Because of the natural structure of plant-based raw materials, AC can be prepared from biomass residues and wastes, including nutshell [8], straw [9], and rice husk [10]. AC is commonly prepared via physical activation or chemical activation [11].

Physical activation requires H_2O or CO_2 and high temperatures. During CO_2 activation, a carbon raw material is reacted with CO_2 at 600-900°C [12]. The preparation of microporous AC by CO_2 activation is relatively mature and is inexpensive. Although this high-temperature activation produces carbon with a high specific surface area, the activity of the raw material is low, the activation time is long, and the pore size distribution is difficult to control [12]. Thus, the quality of the AC is unstable and the mesopores are not well developed, thereby limiting its applications. Comparatively, chemical activation results in higher product yields and requires lower temperatures and shorter activation times, which makes chemical activation more suitable for industrial production. For example, H_3PO_4 activation uses phosphoric acid to impregnate raw materials. Under the protection of inert gas, AC is then produced at 200-600°C [12]. Through chemical activation, good-quality AC with low ash content, low volume shrinkage and low carbon volatilization can be prepared, especially from coconut shells and rice husks. ACs prepared by H_3PO_4 activation have rich distributions of micropores and mesopores, i.e., ideal characteristics for carbon electrodes.

Activation creates and expands pores, thereby improving capacitance. However, during the preparation of biomass-based AC, the cooling process after activation is relatively slow. During this period, the produced micropores and mesopores can completely close up and disappear. Additionally, tar and ash byproducts are not completely removed. These conditions result in decreased pore sizes, pore volumes and surface area and greatly affect the performance of AC.

Plant biomass contains lignin, cellulose and hemicellulose [13]. During physical activation, because of the required high temperatures, cellulose, hemicellulose and lignin gradually pyrolyze and disappear. However, during chemical activation, such as H_3PO_4 activation, lignin is not completely pyrolyzed under the low activation temperatures (below 585°C) and short activation time [14]. The retained lignin becomes an important component of the biomass-based AC. Lignin is a natural high-molecular-weight polymer consisting of randomly polymerized, highly substituted phenylpropane units and has the thermoplastic and glass transition properties of polymer materials [15]. After activation, rapid cooling can quickly change lignin from a high-temperature thermal deformation state to a vitrification state [16,17]. Simultaneously, the pore and pore passages produced by activation are fixed and preserved, unlike the narrowed and contracted passages formed during slow cooling treatments. If the pore structure can be maintained under these low-temperature conditions, then AC prepared at low temperatures and with rapid cooling will have excellent specific surface area, optimal pore sizes and active functional groups. Furthermore, these production conditions will reduce heat and energy requirements and thereby increase potential commercial value.

Through the research we found that lignin did not get full attention. The lignin is completely converted during the general preparation process [10,18,19], and if the lower activation temperature or shorter activation time is used, the conversion is not complete. In addition, the cooling process is carried out slowly under an inert atmosphere [20]. But we found that lignin has thermoelasticity [15] and the gas expands during the activation process to obtain more pore passages and larger specific surface area. If the cooling process is carried out slowly under an inert atmosphere, pore passages will shrink. Comparing to slow cooling process, rapid cooling in liquid nitrogen can reserve pore passages obtained by the expansion of the gas and get a substantial increase in the specific surface area of AC.

In this study, we prepared coconut-shell-based AC by H_3PO_4 activation [21,22,23]. After activation, a rapid cooling method with liquid nitrogen was used. The prepared AC was characterized to determine its pore structure, specific surface area and surface morphology. The prepared AC was also prepared as an electrode to investigate its double-layer capacitive performance via cyclic voltammetry (CV), galvanostatic charge/discharge (GCD) and electrochemical impedance spectroscopy (EIS). The applicability and validity of the rapid cooling method were analyzed and discussed, and the method was subsequently compared with slow cooling methods.

2. EXPERIMENTAL PART

2.1. Preparation of activated carbon

The coconut shells were placed in a laboratory muffle furnace under N_2 flow and carbonized at 450°C for 1h. After carbonization, 20 grams of crude carbons were divided into two equal samples, both of which were well-mixed with 6.8 M H_3PO_4 solution at an impregnation ratio of 2:1 for 1 h. Then, both mixtures were dried at 110°C for 2 h. The activation of both mixtures was carried out in the laboratory muffle furnace under N_2 flow. In the tubular furnace, the temperature was increased at approximately 5°C/min from room temperature to 350°C and maintained at 350°C for 0.5 h. Then, one mixture was removed from the muffle furnace and immediately immersed in liquid nitrogen at -196°C until the liquid nitrogen had evaporated. The other mixture was naturally cooled to room temperature under N_2 flow. Afterward, the two cooled AC products were washed several times with deionized water. Small amounts of concentrated hydrochloric acid were added to remove any ash byproducts. The AC products were then washed with deionized water until pH=7 and subsequently dried. As such, two samples of AC were prepared: AC-1 (by rapid cooling) and AC-2 (by natural cooling). Meanwhile, samples of AC with same process conditions except the activation temperature (500°C , 650°C, 800°C) were prepared.

2.2. Characteristics of activated carbon

The specific surface areas and pore size distributions were analyzed using a specific surface and pore size analyzer (3H-2000PS4). The specific surface area was determined by the Brunauer-Emmett-Teller (BET) method. The pore size distribution was evaluated by the Barrett-Joyner-Halenda (BJH) method. Functional groups on the AC products were analyzed by Boehm titration.

2.3. Preparation of electrodes

AC, acetylene black, and polyvinylidene fluoride were dried at 120°C for 5 h and thoroughly mixed in a mass ratio of 8:1:1, respectively. An appropriate amount of N-Methyl pyrrolidone was subsequently added to prepare a paste-like mixture, and the mixture was uniformly coated onto 150 μm-thick aluminum foil. After drying, the resultant semi-dry electrodes were passed slowly through a

roller machine and vacuum-dried at 120°C for 12 h. As such, two AC electrodes were prepared: ACE-1 (with AC-1) and ACE-2 (with AC-2).

2.4. Electrochemical measurements

The capacitance performances of the electrodes were investigated using CV, GCD and EIS. All electrochemical measurements were performed on a Methohm Autolab in 1 M Na_2SO_4 solution at room temperature using a three-electrode cell. The ACE electrodes were used as the working electrode, a platinum electrode served as the counter electrode, and an Ag/AgCl electrode was used as the reference electrode.

Electrode specific capacitance (C; F/g) was calculated from the cyclic voltammograms according to Eq. (1):

$$C = \frac{\int_{U1}^{U2} I(U)dU}{2 \times \mathrm{m} \times u \times \Delta U} \quad (1)$$

where C, m, u, and ΔU represent the specific capacitance (F/g), the mass of active material in the electrode (g), the scanning rate (V/s) and the potential window (V), respectively. The mass of the active material is equal to the mass of the electrode less the mass of the aluminum foil, multiplied by the ratio of the active material.

The specific capacitance (C; F/g) of the electrodes can also be calculated from the GCD curves according to Eq. (2):

$$C = \frac{I \times \Delta \mathrm{t}}{m \times \Delta U} \quad (2)$$

where I, Δt, and ΔU represent the discharge current (A), the discharge time (s), and the potential interval (V).

3. RESULTS AND DISCUSSION

Table 1. Specific surface area of activated carbon products with different activation temperatures and cooling methods.

Temperature/°C Temperature/℃ Specific surface area /m^2/g Cooling method	Rapid cooling	Natural cooling
350	1176.344	578.224
500	1326.624	1022.079
650	1097.278	1045.509
800	1306.139	1298.312

Table 2. Specific surface area, average pore size, yield and functional groups of activated carbon products.

Sample	AC-1	AC-2
Specific surface area /m^2/g	1176.344	578.224
Average pore size /nm	2.936	2.540
Yield/%	79.88	81.63
$n_{NaOH}/10^{-4}$mol	9.456000	10.140676
$n_{Na2CO3}/10^{-4}$mol	5.176435	7.239306
$n_{NaHCO3}/10^{-4}$mol	8.298250	9.562712
$n_{RCOOH}/10^{-4}$mol	8.298250	9.562712
$n_{RCOOCOR'}/10^{-4}$mol	2.054620	4.915900
$n_{ArOH}/10^{-4}$mol	4.279565	2.901370

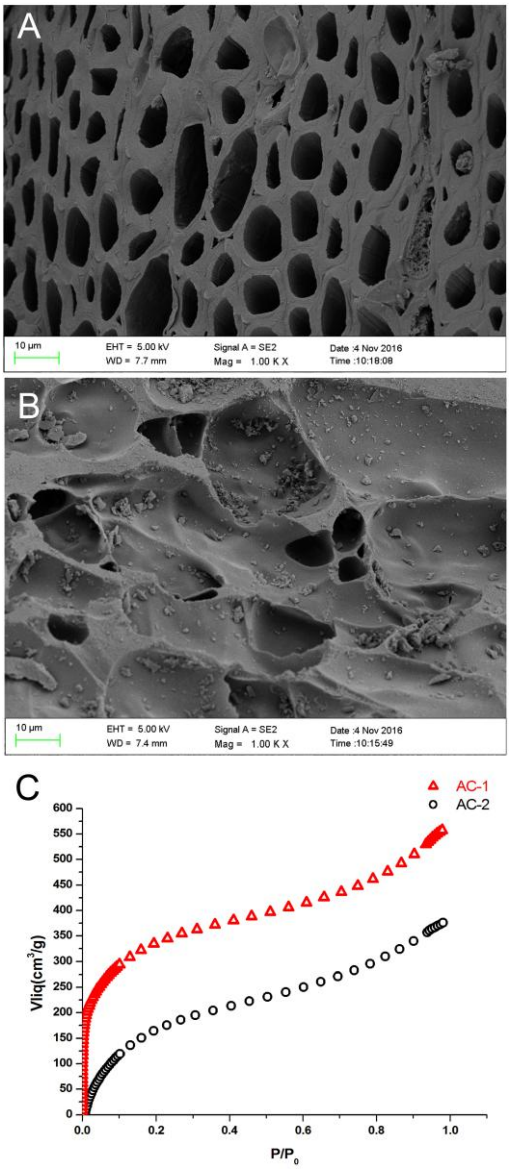

Figure 1. SEM images of AC-1 (A) and AC-2 (B), N_2 adsorption isotherms at -196°C on activated carbon (C).

Table 1 shows specific surface area of ACs with different activation temperatures and cooling methods. Comparing to natural cooling, rapid cooling increased the specific surface area by 103.4% at the activation temperature of 350°C. However, with the raise of activation temperature, the increase in surface area drastically reduced. At the activation temperature of 800°C, rapid cooling increased the specific surface area by 0.6%. That mainly due to the complete decomposition of lignin at high temperatures. Laine's group [8] prepared activated carbons with a specific surface area of 1100.0 m^2/g from coconut shells at 450°C for 1 h using H_3PO_4 activation. Firoozian's group [23] prepared activated carbons with a specific surface area of 1146.3 m^2/g from coconut shells at 700°C for 1 h using H_3PO_4 activation. We are able to obtain activated carbon with a specific surface area of 1176.344 m^2/g at low activation temperatures (350°C) and shorter activation time (0.5h) by rapid cooling, which greatly reduces energy consumption. Table 2 shows specific surface areas, average pore sizes, yields and functional groups of AC-1 and AC-2. The specific surface area of AC-1 was substantially greater than that of AC-2.

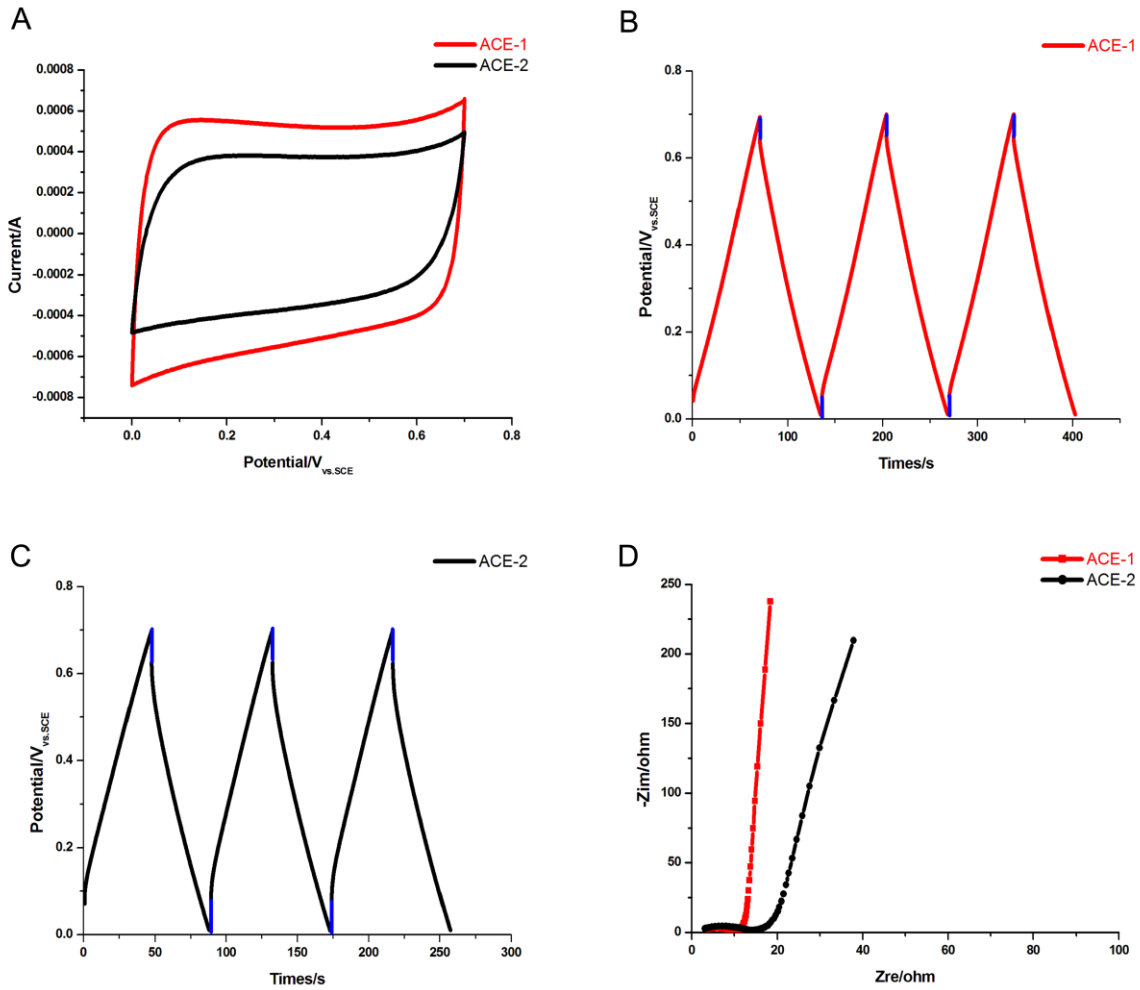

Figure 2. Cyclic voltammetry curves of activated carbon electrodes (ACEs) using a three-electrode cell in 1 M Na_2SO_4 at 5 mV/s (A). Galvanostatic charge-discharge curves of activated carbon electrodes (ACEs) using a three-electrode cell in 1 M Na_2SO_4 at 1 mA (B and C). Electrochemical impedance spectroscopy of activated carbon electrodes (ACEs) using a three-electrode cell in 1 M Na_2SO_4 (D).

Because of the rapid cooling method, the specific surface area increased from 578.224 m^2/g to 1176.344 m^2/g. The average pore size also improved from 2.540 nm to 2.936 nm. During the natural cooling, hydroxy groups which are beneficial to improving the specific capacitance of electrodes [24,25], continuously oxidized and decreased. But the rapid cooling method reduced the oxidation of hydroxyl groups and the number of carboxyl groups and lactone groups, which hinder the charging process of theinterface and affect the electrochemical performance of ACs [25]. Thus, the increase in pore size and the presence of hydroxyl groups can improve the wettability of the surface, increase the effective specific surface area and reduce the resistance to ion transport.

Through rapid cooling, AC-1 maintained a structured state after activation, presenting a smooth and porous active layer. Conversely, in the case of AC-2, a large number of pores were occluded as the temperature gradually decreased during natural cooling, thereby reducing the specific surface area and forming a rough and occluded active layer (Fig. 1A and B). These different cooling methods resulted in ACs with substantially different specific surface areas and pore sizes. Fig. 1C depicts the N_2 adsorption isotherms of the AC products. When the relative pressure was less than 0.2, the amount of N_2 adsorbed sharply increased. When the relative pressure was greater than 0.2, a slow increase was observed. The adsorption curve of AC-1 is characterized as a type I isothermal adsorption curve according to the IUPAC classification [26]. The surfaces of the active layer showed a large number of micropores and mesopores. However, in the case of AC-2, irrespective of the relative pressure, the adsorption growth was relatively slow, with fewer micropores and more mesopores and macropores compared to those of AC-1.

Fig. 2A displays the cyclic voltammetry curves of ACE-1 and ACE-2, where the potential was swept from 0 to 0.7 V vs. SCE at 5 mV/s. The CV curves of both electrodes have an almost rectangular shape, indicating excellent double-layer capacitance performance [27]. Both curves have small humps attributable to redox reactions related to surface active groups such as hydroxy groups. The CV curves also show large specific capacitance increases from 66.06 F/g in ACE-2 to 101.68 F/g in ACE-1 because of the synergistic effects of a larger specific surface area, a greater pore size and more active groups. Both the masses of the active material in ACE-1 and ACE-2 were 0.001 g. Large specific surface areas provide larger numbers of attachment points for ions in solution. Appropriate pore structures facilitate the migration of ions. Additionally, oxygen-containing functional groups increase the wettability of the pores and the effective specific surface area.

Fig. 2B and C illustrate galvanostatic charge-discharge curves for ACE-1 and ACE-2 at 1 mA. When compared with the ACE-2 curve, the ACE-1 curve has better symmetry and stability, indicating an excellent capacitive property and promising performance in continuous power generation. Additionally, a smaller voltage drop appeared in the curve of ACE-1, indicating lower resistance and favorable capacitive characteristics. This was primarily attributed to the appropriate pore structure and hydroxy groups of the AC, which reduced the ion migration resistance. The specific capacitance of ACE-1 and ACE-2 calculated by this way are 100.55 F/g and 65.26 F/g respectively, which are roughly equal to the results calculated by CV.

Fig. 2D shows the EIS curves for ACE-1 and ACE-2, with a ±5 mV potential amplitude and covering the frequency range from 10 mHz to 10 kHz. Under ideal conditions, the impedance curve is a straight line perpendicular to the horizontal axis. However, for actual porous electrodes, because of

the presence of contact resistance, charge-transfer impedance and Warburg impedance, the curve appears as a semicircle and a curve [28]. In Fig. 2D, a comparison of the curve for ACE-1 with that for ACE-2 reveals that ACE-1 has a lower resistance. The ACE-1 curve is in the high-frequency region, which is closer to the ideal conditions, indicating better capacitance characteristics. The ACE-1 exhibited improved surface wettability and reduced ion migration resistance because of the well-defined pore structure and hydrophilic oxygen-containing functional groups.

4. CONCLUSIONS

When compared with natural cooling, this rapid cooling method effectively improved the properties of the AC and carbon electrodes. The number of micropores greatly increased, pore sizes expanded obviously, and the specific surface area increased by 103.4%. These effects resulted in the specific capacitance of carbon electrodes increased by 53.9%. Furthermore, reductions in the numbers of carboxyl and lactone groups and increases in the number of hydroxyl groups improved the specific capacitance.

Under the same activation conditions and inert cooling atmosphere, the effect of rapid cooling with liquid nitrogen is better than the slow cooling with nitrogen. However, as the activation temperature increases, the effect of rapid cooling with liquid nitrogen reduced. Therefore, the rapid cooling method is suitable for low temperature activation conditions to obtain larger specific surface area. But for the ultra-large surface area of activated carbon, the effect is not obvious.

ACKNOWLEDGEMENTS
This work was supported by the “Chunhun Plan” of Ministry of Education PRC (z2016096), the Key Laboratory for Biomass Gasification Technology of Shandong Province, the Natural Science Foundation of Shandong Province (ZR2016YL007) and the Special Fund for Agro-scientific Research in the Public Interest (201503135-04).

References

1. S. Muthu and S. Y. Narahari, *Electrochemical capacitor*, 55 (2007) 7479.
2. F. Lufrano, P. Staiti, E.G. Calvo, E. J. Juarez-Pere, J. A. Menéndez, A. Arenillas, *Int. J. Electrochem. Sci*., 6 (2011) 596.
3. X. F. Sun, Y. L. Xu, J. Wang, S. C. Mao, *Int. J. Electrochem. Sci.*, 7 (2012) 3205.
4. R. Farma, M. Deraman, Awitdrus, I. A. Talib, R. Omar, J.G. Manjunatha, M. M. Ishak, N. H. Basri1 and B. N. M. Dolah, Int. J. Electrochem. Sci., 8 (2013) 257.
5. J. M. V. Nabai, J. G. Teixeira and I. Almeida, J. *Bioresour. Technol*., 102 (2011) 2781.
6. A. Elmouwahidi, Z. Zapatabenabithe, F. Carrascomarin and C. Morenocastilla, J. *Bioresour. Technol*., 111 (2012) 185.
7. T. F. Huang, Z. H. Qiu, D. W. Wu, Z.B. Hu, *J. Int. J. Electrochem. Sci*., 10 (2015) 6312.
8. J. Laine, A. Calafat and F. C. Severino, *Biennial Conference on Carbon*, Worcester, MA, USA, 1987, 334.
9. Y. H. Ma, *Waste Biomass Valor*, (2016) 1.

10. S. B. Daffalla, H. Mukhtar and M. S. Shaharun, *Int. J. Global Environ. Issues*., 12 (2012) 107.
11. Y. Sudaryanto, S. B. Hartono, W. Irawaty, H. Hindarso and S. Ismadji, J. *Bioresour. Technol*., 97 (2006) 734.
12. L. M. Sun, L. P. Zhang, J. H. Xue and B. Z. Li, J. *Chemistry Bioengineering*, 33 (2016) 5.
13. V. Pasangulapati, K. D. Ramachandriya, A. Kumar, M. R. Wilkins, C. L. Jones and R. L. Huhnke, J. *Bioresour. Technol*., 114 (2012) 663.
14. H. Cheng, J. Yu, M. Q. Yao and G. W. Xu, *Ciesc Journal*, 64 (2013) 1757.
15. L. Cheng, H. P. Cheng, Q. Lu, S. J. Ding, X. H. Wang and M. P. Yang, *Ciesc Journal*, (2014) 3626.
16. Tsujiyama S, J. *Scientific Reports of the Kyoto Prefectural University Agriculture*, 47 (1995) 43.
17. Hatakeyama, H and Hirogaki, A, J. *Therm. Anal. Calorim.*, 114 (2013) 1075.
18. Suhas, P. J. M. Carrort, M. M. R. Carrott, J. *Bioresour. Technol*., 98 (2007) 2301.
19. Y. Uraki, R. Taniwatashi, S. Kubo, Y. Sano, *J. Wood. Sci*., 46 (2000) 52.
20. M. K. B. Gratuito, T. Panyathanmaporn, R. A. Chumnanklang, N. Sirinuntawittaya, A. Dutta, J. *Bioresour. Technol*., 99 (2008) 4887.
21. M. J. Prauchner, F. R. Reinoso, J. *Microporous Mesoporous Mater*., 152 (2012) 163.
22. R.B. Rios, F. W. M. Silva, A. E. B. Torres, D. C. S. Azevedo, C. L. C. Jr, *Adsorption*, 15(2009), 271.
23. P. Firoozian, I. U. H. Bhat, H. P. S. A. Khalil, A. M. Noor and A. H. Bhat, *Mater. Technol*., 26 (2011) 222.
24. D. U. Xuan, C. Y. Wang, Z. Q. Shi and C. Y. Guo, *J Tianjin Univ*, 39 (2006) 1479.
25. L. Z. Fan, S. Qiao, W. Song, M. Wu, X. He and X. Qu, *Electrochim. Acta*, 105 (2013) 299.
26. K. S. W. Sing, M. *Handbook of Heterogeneous Catalysis*. Wiley- VCH Verlag GmbH & Co. KGaA, (1984) London, Great Britain.
27. A. Velikonja, V. K. Iglic, A. Iglic, *Int. J. Electrochem. Sci*., 10 (2015) 1.
28. X. Z. Sun, B. Huang, X. Zhang, D. C. Zhang, H. T. Zhang and Y. W. Ma, *Acta Physico-Chimica Sinica*, 30 (2014) 2071.